High Resolution Analysis of Follicular Lymphoma Genomes Reveals Somatic Recurrent Sites of Copy-Neutral Loss of Heterozygosity and Copy Number Alterations that Target Single Genes

K-John J. Cheung,[1]* Allen Delaney,[2] Susana Ben-Neriah,[1] Jacquie Schein,[2] Tang Lee,[1] Sohrab P. Shah,[1] Dorothy Cheung,[2] Nathalie A. Johnson,[1] Andrew J. Mungall,[2] Adele Telenius,[1] Betty Lai,[1] Merrill Boyle,[1] Joseph M. Connors,[1] Randy D. Gascoyne,[1] Marco A. Marra,[2] and Douglas E. Horsman[1]

[1]Center for Lymphoid Cancer, British Columbia Cancer Agency, Vancouver, BC
[2]Genome Sciences Center, British Columbia Cancer Research Center, Vancouver, BC

A multiplatform approach, including conventional cytogenetic techniques, BAC array comparative genomic hybridization, and Affymetrix 500K SNP arrays, was applied to the study of the tumor genomes of 25 follicular lymphoma biopsy samples with paired normal DNA samples to characterize balanced translocations, copy number imbalances, and copy-neutral loss of heterozygosity (cnLOH). In addition to the t(14;18), eight unique balanced translocations were found. Commonly reported FL-associated copy number regions were revealed including losses of 1p32-36, 6q, and 10q, and gains of 1q, 6p, 7, 12, 18, and X. The most frequent regions affected by copy-neutral loss of heterozygosity were 1p36.33 (28%), 6p21.3 (20%), 12q21.2-q24.33 (16%), and 16p13.3 (24%). We also identified by SNP analysis, 45 aberrant regions that each affected one gene, including *CDKN2A, CDKN2B, FHIT, KIT, PEX14*, and *PTPRD*, which were associated with canonical pathways involved in tumor development. This study illustrates the power of using complementary high-resolution platforms on paired tumor/normal specimens and computational analysis to provide potential insights into the significance of single-gene somatic aberrations in FL tumorigenesis.

INTRODUCTION

Approximately 85% of follicular lymphoma (FL) cases are associated with a specific balanced translocation, t(14;18)(q32;q21), that leads to over expression of the antiapoptotic gene *BCL2* due to its relocation in proximity to an *IGH* enhancer element (Tilly et al., 1994). This genetic abnormality alone, however, is unlikely to produce clinical FL, as BCL2 over-expressing transgenic mice do not develop lymphoma (McDonnell et al., 1989; McDonnell and Korsmeyer, 1991) and t(14;18)-bearing lymphocytes have been frequently demonstrated in lymphoid tissue or blood of healthy individuals (Limpens et al., 1995; Dolken et al., 1996). It has, therefore, been hypothesized that the acquisition of secondary genetic alterations following the initial t(14;18) event will be necessary for full disease manifestation.

The reported recurrent copy number alterations detected by karyotype analysis, comparative genomic hybridization (CGH) or array CGH have consistently included losses of 1p32-36, 6q, 9p, 10q, and 17p, and gains of 1q, 2p, 7, 12, 18q, and X (Bende et al., 2007; Ross et al., 2007; Cheung et al., 2009). However, these regions were generally very large (over 500 kb) and contained too many genes to allow identification of specific candidate genes associated with disease initiation and progression. In this study, we have used a combination of conventional cytogenetic techniques, genome-wide tiling path BAC array CGH and Affymetrix 500K single nucleotide polymorphism (SNP) arrays to investigate a cohort of 50 specimens derived from 25 FL tumor samples and 25 matched normal tissues, with the goal of (1) identifying all copy number aberrations

Additional Supporting Information may be found in the online version of this article.

Supported by: Terry Fox Foundation New Frontiers Program Project Grant, Grant number: 016003; National Cancer Institute of Canada, Grant number: 019005; Michael Smith Foundation for Health Research, Grant number: ST-PDF-01793; Canadian Institute of Health Research, Grant number: STP-53912; National Cancer Institute of Canada, Genome Canada/BC Grant Competition III, Terry Fox Young Investigator and Michael Smith Senior Research Scholar.

*Correspondence to: K-John J. Cheung, British Columbia Cancer Agency, 600 West 10th Avenue, Vancouver, British Columbia V5Z4E6, Canada. E-mail: kjcheungjr@bccancer.bc.ca

Received 26 October 2009; Accepted 22 March 2010

DOI 10.1002/gcc.20780

Published online 26 April 2010 in Wiley InterScience (www.interscience.wiley.com).

including those that would otherwise escape the detection capability of lower resolution array platforms, (2) detecting copy-neutral loss of heterozygosity (cnLOH) events, and (3) using computational analysis to focus on single genes affected by small regional aberrations. The use of paired tumor and normal samples in the analysis of copy number aberrations and cnLOH allows for the detection of somatic changes while masking common polymorphic variants and for precise calling of LOH in comparison to analysis performed using tumor-only LOH with inference from reference controls. The resolution of the 500K SNP platform is the highest that has been reported for interrogating this disease with paired tumor/normal specimens. This study specifically focuses on examining the significance of single genes in areas of alteration that have not been detected by other methods.

MATERIALS AND METHODS

Patient Materials

The 50 study specimens were accessioned between 2004 and 2008 at the British Columbia Cancer Agency in Vancouver, British Columbia, in a prospective accrual that included a lymph node biopsy paired with a peripheral blood sample or flow sorted nonclonal lymphocytes obtained from the biopsy specimen to be used as a source of constitutional patient DNA. The acquisition of these samples was undertaken for the investigation of the lymphoma tumor genomes through BAC library construction and BAC fingerprint analysis (National Cancer Institute of Canada). The details of the BAC fingerprinting investigations are being reported elsewhere. The data in this report describe a subset of the comprehensive multiplatform analysis that was being performed on these lymph node specimens.

The tissue specimen requirements for inclusion in the study included fresh or fresh frozen tissue showing FL morphology in a diagnostic or follow-up lymph node biopsy with a >50% tumor content that could be subjected to purification of the tumor cells by flow sorting (two patients had sufficiently high tumor content that their samples did not undergo the sorting process). These patient specimens had to meet three criteria: (1) a diagnosis of follicular lymphoma based on the criteria defined by the World Health Organization classification of tumors of hematopoietic and lymphoid tissues (Swerdlow et al., 2008), (2) sufficient tumor cell content in the lymph node biopsy (~400 million cells in suspension with the goal of obtaining 40–50 million live purified CD19 light chain restricted cells), and (3) availability of matched normal peripheral blood or sufficient nontumor sorted cells to obtain control normal DNA for use in the Affymetrix and array CGH studies. Study-specific consent protocols were used for the collection of normal DNA and occasionally a second lymph node biopsy. This study was approved by the University of British Columbia IRB and was performed in accordance with the Declaration of Helsinki.

Cytogenetic Analysis

Cytogenetic analysis of lymph node specimens was performed as previously described (Horsman et al., 2001). Fluorescence in situ hybridization (FISH) was performed using the LSI *IGH/BCL2* probe (Abbott, Downers Grove, IL) for detection of the *IGH/BCL2* genomic fusion, the RP11-454C15 or RP11-149I2 BAC probe or the WI2-2846G20 fosmid probe for 9p21 deletions, and the RP11-794O16 or RP11-1069N18 BAC probe for 10q23.33 deletions. The RP11-47M15 or RP11-525G07 probe at 9q31 or 9q33 and the RP11-379O18 probe at 10p12.2 served as controls for copy number.

Cell Sorting and Sample Preparation

All but two lymph nodes selected for array CGH and 500K SNP array analyses were fluorescence-activated-cell sorted using fresh cell suspensions to collect CD19 positive, light chain restricted cells from the biopsy specimens to achieve tumor content in the range of 95–99%. Sample preparation was performed as previously described (Johnson et al., 2009).

BAC and SNP Arrays

The submega base resolution tiling (SMRT) array contains 26,819 BAC clones spotted in duplicate and covers >95% of the human genome (Ishkanian et al., 2004; Krzywinski et al., 2004). The array CGH analysis was performed as previously described (de Leeuw et al., 2004). The Affymetrix GeneChip 500K SNP array set was performed using 500 ng samples of tumor and constitutional DNA according to manufacturer's protocol (Affymetrix, Santa Clara, CA).

Computational and Statistical Analyses

Scoring of array CGH data was performed using the Hidden Markov Model (HMM) program CNA-HMMer v0.1 (available at http://www.cs.ubc.ca/~sshah/acgh/) as described previously (Shah et al., 2006, 2007; Cheung et al., 2009). For SNP analysis, raw intensity data from Affymetrix were imported into Partek Genomic Suite software (Partek Incorporated, St. Louis, MO) and analyzed using the genomic segmentation tool for copy number detection. A minimum of 10 markers were specified, whereas the *P* value threshold and the signal-to-noise ratio were set at 0.001 and 0.6, respectively, to give a balance of sensitivity and specificity. Multiple test corrections were performed using the Benjamini and Lui stepdown method with an alpha value of 0.05 (Benjamini and Liu, 1999). cnLOH analysis was performed using genotype calls derived from microarray images using the GTYPE v4.0 software program (Affymetrix, Santa Clara, CA). The analysis of cnLOH was a measure of change from heterozygous in the constitutional to homozygous in the tumor samples. For plotting and breakpoint detection, a heterozygous allele was given a score equivalent to copy number 2, and a homozygous allele a score equivalent to copy number 1. SNPs which were observed to be homozygous in the constitutional DNA were not used in this analysis. Ingenuity pathways analysis software (Ingenuity® Systems, www.ingenuity.
com) was used to examine 40 genes identified by the 500K SNP arrays for their relevance to currently known biological functions and canonical pathways. *P* values are calculated with the right-tailed Fisher's Exact Test and $P \leq 0.02$ indicates a statistically significant, nonrandom association. The Benjamini-Hochberg multiple testing correction was also used where appropriate.

RESULTS

Clinical Data

All cases had the standard morphological and immunophenotypic characteristics of FL. Eighteen of 25 cases were male, and the median age of the cohort was 56 years. Thirteen cases were diagnosed as FL grade 1, seven were grade 2, and five were grade 3A. Of the 25 patients, two developed histological transformation to diffuse large B cell lymphoma.

Cytogenetic Data

Twenty-one of the 25 cases were studied by karyotype analysis. Four cases were not investigated by karyotype analysis due to failure to obtain metaphases or nonsubmission of fresh tissue for culture. Supporting Information Table 1 shows the karyotype details and the total number of aberrations and balanced translocations for each specimen. The median number of aberrations per case was three (range 0 to 13 aberrations). The t(14;18) was present in 20 of these 21 cases (95.2%); the remaining case displayed no abnormal cytogenetic features. Nine apparently balanced translocations other that the t(14;18) were detected. One of these was a three-way translocation t(1;11;3). A number of them were resolved by multicolor karyotyping and the breakpoint site on one or both partner chromosomes was uncertain. A t(3;16)(q27;p13) has previously been reported by ourselves and others in FL (Horsman et al., 2001) and DLBCL (Au et al., 1999; Sanchez-Izquierdo et al., 2001; Johnson et al., 2008). t(2;4)(p16;q28) and t(2;4) have been described in DLBCL by Barbieri et al. (1984) and Mecucci et al. (1983), respectively, but whether these represent an identical translocation to the t(2;4)p?;q2?8) we describe cannot be stated with any certainty. Otherwise, a search of the online Mitelman Database of Chromosome Aberrations in Cancer (http://cgap.nci.nih.gov/Chromosomes/AbnCytSearchForm) did not reveal similar balanced translocations to those indicated (underlined and bolded) in Supporting Information Table 1 in either follicular lymphoma or diffuse large B-cell lymphoma categories.

FL-Associated Copy Number Alterations

Genome-wide analysis was performed using both BAC array CGH and the 500K SNP array. In each analysis, copy number profiles of the 25 FL cases were combined to generate a composite frequency ideogram with all aberrations affecting the 22 autosomes and the X chromosome (Figs. 1A and 1B). BAC array CGH data from the 25 FL samples with matched normal specimens were analyzed computationally using the program CNA-HMMer v0.1. Supporting Information Table 2 shows the details of the 110 somatic copy number alterations (80 gains and 30 deletions) that were recurrent in two or more cases. For the SNP array analysis, the genomic segmentation algorithm from Partek software produced 180 regions of somatic aberration in two or more

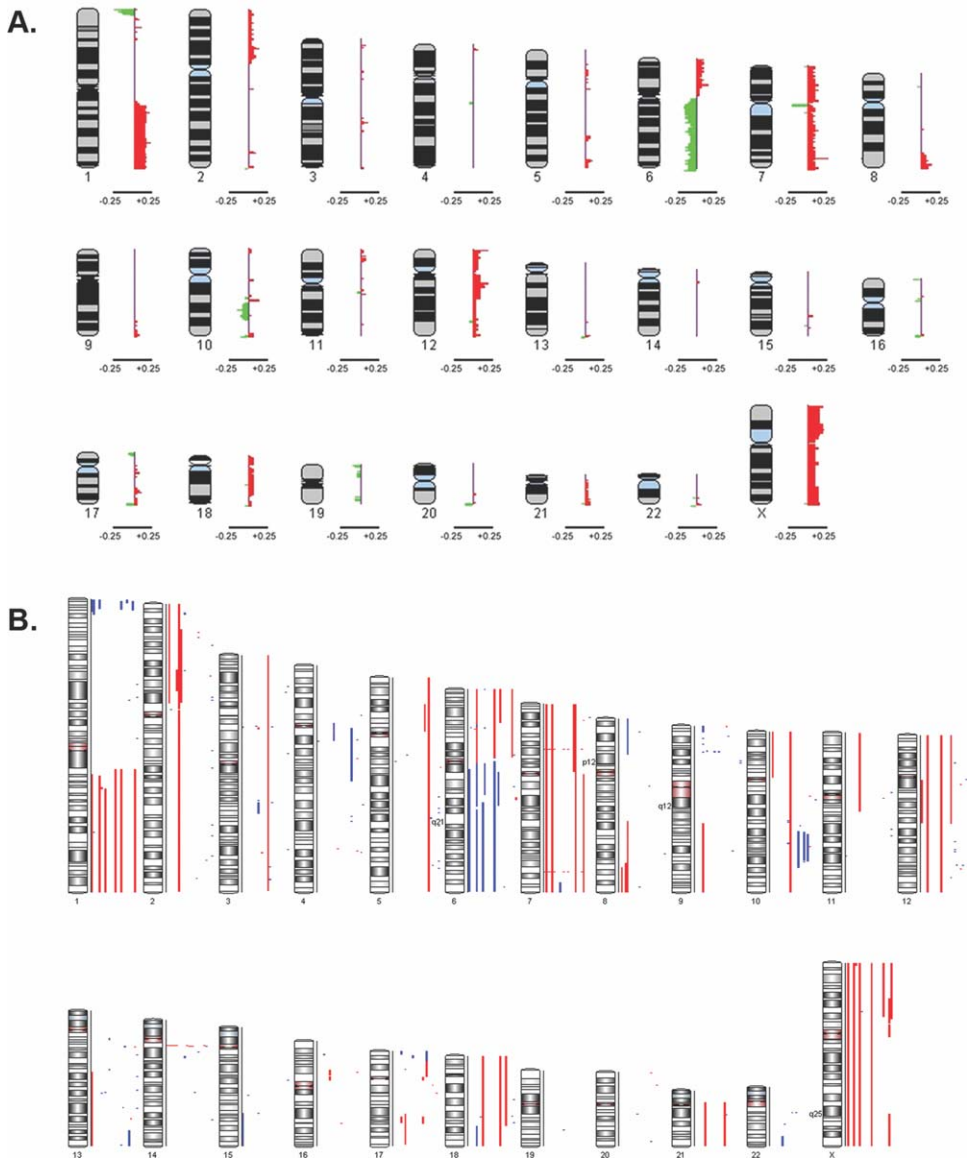

Figure 1. Copy number alterations in 25 FL cases with matched normal specimens. A: Copy number profiles of the 25 FL cases were combined to generate a composite frequency ideogram with all aberrations affecting the 22 autosomes and the X chromosome. Green and red signals represent losses and gains, respectively. The horizontal bar below each ideogram represents gain and loss frequencies of +0.25 and −0.25, respectively. B: Composite copy number profiles of the 25 tumor/normal paired samples were analyzed using the Affymetrix 500K SNP array set. Copy number frequencies were generated by Partek software using the genomic segmentation algorithm. Genetic losses or gains are represented by blue and red signals, respectively.

cases after adjusting for multiple test corrections (Benjamini and Lui stepdown method with an alpha value of 0.05; Supporting Information Table 3). Of the 298 aberrations, 126 were gains and 172 were deletions. Table 1 shows the distribution of deletions versus gains detected by each platform. The majority of the aberrations were less than 5 Mb and, therefore below the resolution of cytogenetic analysis. The lower resolution of BAC array when compared with the 500K SNP array is clearly reflected in its ability to only detect gain of amplified regions greater than ~180 kb in size and deletions greater than ~140 kb, whereas the 500K SNP array was able to identify gains as small as ~3.0 kb and deletions ~7.0 kb in size, respectively. The concordance percentages, defined as the proportion of those aberrations detected by array CGH that corresponded to those by SNP array, for gained and deleted regions between the two platforms, were 87% and 84%, respectively. The most frequently altered regions revealed by either platform, other

TABLE 1. Distribution of Deletions and Gains in Tiling BAC Array CGH and the 500K SNP Array Set

	BAC CN	SNP CN
No. gains	80	126
Size range (bp)	178,189–103,119,662	2,994–247,135,060
No. deletions	30	172
Size range (bp)	142,911–108,533,179	6,888–231,187,823

CN, copy number.

than functional immunoglobulin and T-cell receptor rearrangements, were 1p36 terminal deletion, gain affecting chromosome arm 1q, and gain of the X chromosome, all showing >20% frequency of alteration. These were followed by other commonly reported regions such as gains of 6p, 7, and 12 and losses of 6q and 10q.

In comparing the positions of SNP-detected copy number imbalances to the karyotype-defined breakpoints of nine detected balanced translocations, one apparently balanced translocation, t(10;13)(q24;q12) in Case ID no. 16, revealed localized deletions at 10q23.32-q23.33 (93,738,383–94,945,929 bp) and 13q12.12-q12.13 (22,690,184–24,527,050 bp). Genes included in these regions were *BTAF1*, *CPEB3*, *CYP26A1*, *CYP26C1*, *EXOC6*, *HHEX*, *IDE*, *KIF11* and *MARCH5*, and *ATP12A*, *C1QTNF9*, *CENPJ*, *LOC646405*, *MIPEP*, *PARP4*, *PCOTH*, *RNF17*, *RP11-45B20.2*, *SACS*, *SGCG*, *SPATA13* and *TNFRSF19*, respectively. Three other cases have large deletions at 10q (spanning from 10q23.1-q25.1) that included the 10q23.32-q23.33 microdeletion (and therefore the genes within it) of Case ID no. 16, whereas no other cases overlapped with the 13q microdeleted region. Lastly, no deletions or duplications were seen at the presumed breakpoint sites of the other balanced translocations.

FL-Associated Copy-Neutral LOH

The 500K SNP array set was used to interrogate the 25 FL biopsies for cnLOH. A total of 36 regions affecting chromosomes 1, 2, 3, 4, 5, 6, 9, 10, 12, 15, 16, 17, and 19 were detected as cnLOH (Fig. 2A). The median size of these alterations was 26.03 Mb (range 1.29 to 142.80 Mb). Of the 25 cases, 19 (76%) displayed at least one region of cnLOH, whereas 11 cases (44%) displayed two or more. Only a minority of the cnLOH aberrations (4/36, 11%) were interstitial. Supporting Information Table 4 provides details of each aberration including the heterozygous rates for tumor and matched normal samples. The four most frequently altered regions were 1p36.33 (7 of 25 cases, 28%), 16p13.3 (6 cases, 24%), 6p21.3 (5 cases, 20%), and 12q21.2-q24.33 (4 cases, 16%). Figure 2B shows representative profiles of allelic imbalances and copy number changes in each of these regions.

Sensitivity of Aberration Detection by Array CGH and 500K SNP

Aberrant regions found by array CGH generally corresponded to those by 500K SNP analysis. Commonly recurrent aberrations associated with FL exhibited the highest correlation between the two platforms. Figure 3A shows representative examples of the proximal 12q gain (left panel), loss of 1p36 with gain of nearly the entire 1q arm (middle panel), and loss of the 10q23-q24 area (right panel; in this case the proximal region of this area is also lost). In areas where the aberrations were small, especially those that spanned only one or two BAC's, or where ambiguity existed due to nonuniform shift of BAC's in the region (overlapping BACs in the area not showing the same degree of shift), computational calls of array CGH data were often not made. However, many of these areas displayed a pattern that corresponded to an alteration detected by the 500K SNP data, which generally had more data points (SNPs) in these regions. The 500K SNP data were able to verify many of these regions, which partly explains the higher frequency of aberrations detected by the 500K SNP compared with array CGH analyses. A number of examples of the inability of the computational analysis to identify single BAC shifts or ambiguous regions in array CGH are shown in Figure 3B. In each case, the high coverage by SNP probes allowed for the verification of subtle BAC array CGH shifts and many of the small regions that contained only one or two genes, thereby facilitating the efforts of gene localization and the analysis of their potential importance in the evolution of disease. *TCRG*, the T-cell receptor gamma gene, was included here for visual comparison but was removed from subsequent analyses as it is known to reflect functional *TCRG* deletion in the T-cell rich nonclonal sorted cells used as the control DNA in this case. Shown in Figure 3C are representative FISH-validated cases with 9p21 and 10q23.3 deletions, two of the regions associated with relatively high frequencies of copy number aberrations detected by the SNP arrays. Of interest, three of the four cases with array-detected

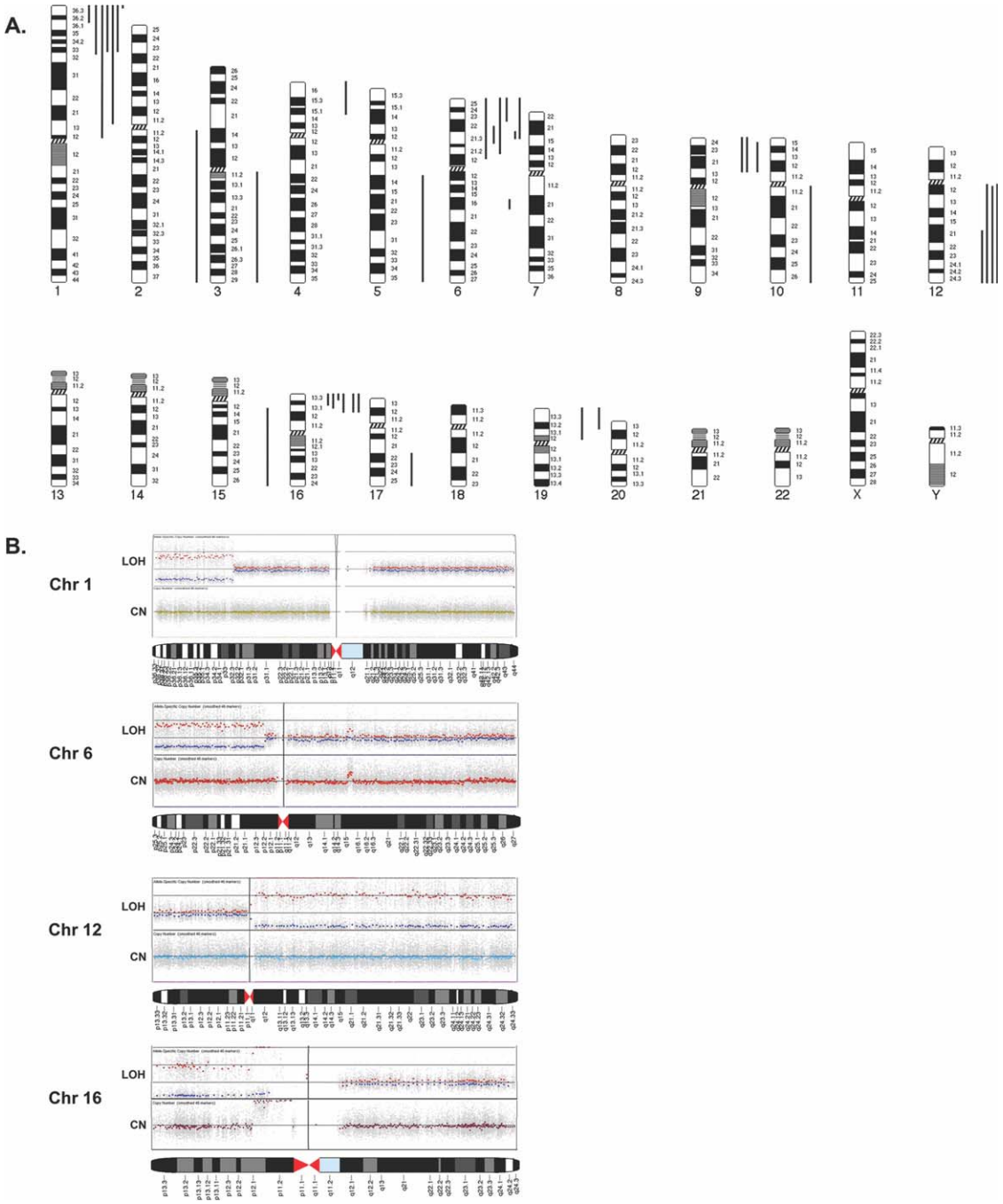

Figure 2. Copy-neutral LOH alterations in 25 FL cases with matched normal specimens. A: A composite frequency plot was generated where black vertical lines represent regions of cnLOH. B: Comparison between the cnLOH (upper panel) and copy number (lower panel) profiles in each of the four regions, 1p36.33, 6p21.3, 12q21.2-q24.33, and 16p13.3, is shown. The blue and red dots at each position along the chromosome in the LOH plot represent the two alleles. The dots of different colors in each of the four chromosomes in the CN (copy number) plot correspond to different specimens. A classical cnLOH pattern is demonstrated by the loss of one allele (a shift downward from the center line) and the gain of the remaining allele (an equal amount of shift upward from the center line), whereas the copy number of the region does not display any shift from the center.

9p21 deletions of variable sizes displayed homozygous deletions. Two of these cases had the smallest 9p21 deletions measuring 123,510 bp and 204,909 bp in size and corresponded to the location of the *CDKN2A/2B* locus. The four cases with 10q23.3 deletions were all heterozygous by FISH analysis, with the smallest measuring 1,380,294 bp in size and corresponded to an area

encompassing 10 genes, including *CYP26A1*, *IDE*, *HHEX*, *FER1L3*, *CPEB3*, *MARCH5*, *EXOC6*, *KIF11*, *CYP26C1*, and *BTAF1*. Further validation by FISH analysis was undertaken for numerous other regions of alteration (data not shown). These data confirm that microdeleted or gained regions represented by a shift from baseline of a single or a few adjacent BACs, and verified by 500K SNP analysis, are frequent features in FL.

Single Genes Affected by Regional Aberrations

While the majority of the copy number aberrations from the SNP array data contained either no genes or multiple genes, 45 (15%) altered regions were identified that each contained a single gene (Table 2; of note, we classified the deleted region that encompasses both *CDKN2A* and *CDKN2B* as a single-gene containing region as they are physically positioned adjacent to one another and have been shown to be frequently deleted and methylated in combination) (Krug et al., 2002). Of these 45 regions, 14 represented regions of gain, whereas 31 were regions of deletion which ranged from 6346 bp to 2.3 Mb in size. Twenty-eight were less than 150 kb in size, the theoretical resolution limit of BAC array CGH analysis using the SMRT array. Supporting Information Table 5 shows the functional information of the 40 unique genes derived from these 45 altered regions. Of these single genes, four (*CDKN2A*, *FHIT*, *KIT*, and *PTPRD*) recurred in two or more cases. In Figure 3D, representative examples of single genes affected by SNP-detected microalterations are shown. We observed that some alterations were small enough that only specific structural regions of the genes were affected. For instance, the 5′ portion of the *KIT* gene appeared to be deleted, whereas the 3′ end was gained. Similarly, the first intron of *FHIT* was deleted but the 3′ end which included the last intron and exon was gained. It is interesting to note that the majority of these single gene regions (39 of 45 regions, 87%) did not fall within the commonly reported areas of alteration in FL, which include losses of 1p32-36, 6q, 10q, and 17p, and gains of 1q, 2p, 6p, 7, 9p, 12, 17q, 18q, and X (Cheung et al., 2009).

Pathway Analysis Using Single Genes Affected by Copy Number Regions

Although genomic regions that show recurrent alterations in multiple cases may indicate biological significance, we postulated that the development of FL or other types of neoplasia is driven by secondary genetic alterations affecting a variety of genes that participate in the same critical pathways. We first performed functional analysis using Ingenuity Pathways Analysis software on the single genes affected by the 45 regional aberrations. Supporting Information Table 6 shows that four biological function categories (cancer, cellular growth and proliferation, cell death, and hematological disease) were significantly associated with the genes in our data set after adjusting for false discovery (Benjamini-Hochberg multiple testing correction, $P \leq 0.02$). The specific genes associated with each functional category are also listed. Further analysis was performed on the single genes to examine their association with known canonical pathways. Two pathways that emerged as significant in our analysis were the Wnt/β-catenin signaling and the G1/S checkpoint regulation pathways (right-tailed Fisher's Exact Test, $P \leq 0.02$) and the genes associated with each pathway are listed in Supporting Information Table 7. Other details of these Ingenuity-curated pathways, including the total genes associated with the Wnt/β-catenin signaling and the G1/S checkpoint regulation pathways and the publication source, are provided in Supporting Information.

DISCUSSION

One of the advantages of combining the tiling path BAC array with the 500K SNP array data are that the BAC probes provide near complete coverage of the genome, whereas the SNP array set increases the resolution in most areas of the genome with a median physical distance between SNP probes of 2.5 kb. This provides an estimated resolution of 25 kb or less when a minimum of 10 SNPs are used to determine an aberration, as undertaken in this study. The other advantage relates to cross validation of results generated from both techniques. Although most BACs in this array average 100 kb in size and the minimum scorable aberration by visual annotation was three contiguous probes showing an obvious shift from the center line (making the functional resolution to be $\geq$300 kb), single BAC shifts that would not be scored computationally or visually may be used to validate small aberrations detected by the SNP array. Thus, the higher resolution data obtained by this combined analysis was used to define multiple single gene lesions

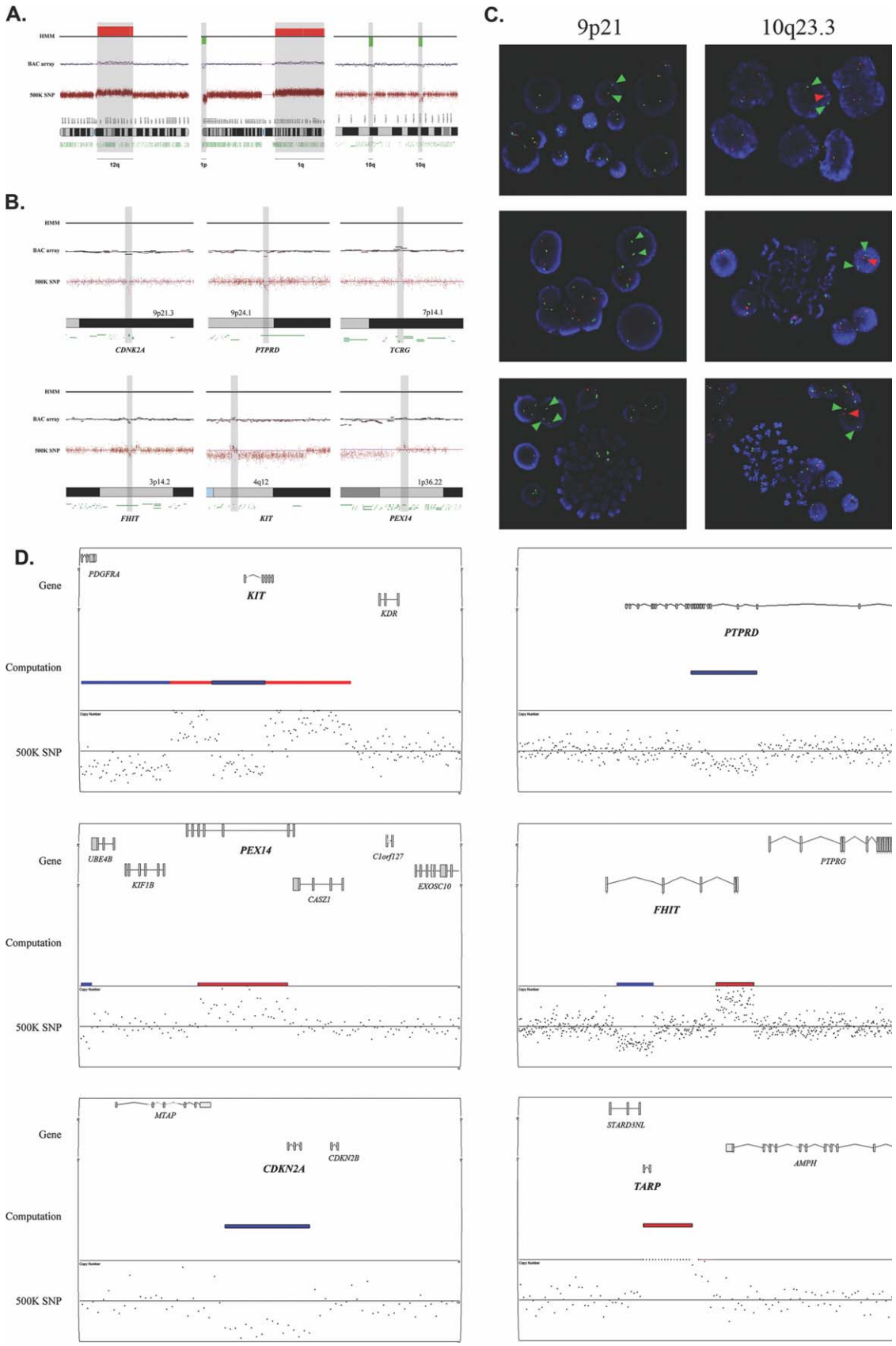
A.
HMM
BAC array
500K SNP
12q
1p
1q
10q
10q
B.
HMM
BAC array
500K SNP
9p21.3
9p24.1
7p14.1
CDNK2A
PTPRD
TCRG
HMM
BAC array
500K SNP
3p14.2
4q12
1p36.22
FHIT
KIT
PEX14
C.
9p21
10q23.3
D.
Gene
Computation
500K SNP
PDGFRA
KIT
KDR
PTPRD
UBE4B
KIF1B
PEX14
CASZ1
C1orf127
EXOSC10
PTPRG
FHIT
MTAP
CDKN2A
CDKN2B
STARD3NL
AMPH
TARP

Figure 3

that were considered in the pathway analysis (see below).

In addition to the previously reported common aberrations of FL, such as t(14;18), 1p deletion, 1q duplication, 6p deletion, and trisomy 7, we identified a comprehensive profile of cnLOH at a density of >500,000 SNP probes. The cnLOH represents a genomic abnormality in which no net change in copy number occurs (Fitzgibbon et al., 2007; Tyybakinoja et al., 2008). We observed that the majority of the cnLOH aberrations were relatively large (median size >26 Mb) and involved either whole chromosomal arms or terminal regions, whereas four were interstitial. Many of the cnLOH detected in our study corresponded to regions that affected by copy number imbalances, highlighting the possibility that neoplastic cells use not only deletions and gains of genetic material to deregulate genes but also the cnLOH mechanism to produce homozygosity for a pre-existing tumor somatic mutation. For example, of the 25 cases, six cases displayed copy number loss of 1p36, whereas seven other cases showed cnLOH at the 1p terminus. Together, 52% of the cases had one or the other aberration at 1p, constituting the most frequent secondary genetic abnormality in FL. The second most frequently altered region was 6p (44% of cases; five with gain and six with cnLOH), followed by 12q (16%; six with gain and four with cnLOH). These findings are in agreement with those of previous SNP array studies (Fitzgibbon et al., 2007; Ross et al., 2007). It is interesting to note that 16p is the only region where copy number alterations rarely occurred but cnLOH was detected in six cases (24%). As the smallest overlapping cnLOH area still measured 3.8 MB, containing over 40 genes, further studies are needed to understand the lymphomagenic significance of this region in FL. Also of interest was the 9p21 region, where two cases with FISH-validated homozygous single-gene deletions also displayed cnLOH, illustrating the use of the cnLOH mechanism to inactivate genes by duplication of existing somatic deletions.

Due primarily to the resolution of our array platform and the use of matching constitutional DNA (therefore eliminating the application of algorithms that study runs of homozygosity), our SNP analysis was able to generate regions of cnLOH that were smaller in size compared with previous studies. For instance, the three smallest cnLOH-rich regions on 1p, 6p, and 16p were 4.8, 1.3, and 3.8 Mb compared with ≥9 Mb in three past reports of follicular lymphoma (Fitzgibbon et al., 2007; Ross et al., 2007; O'shea et al., 2009). In terms of copy number imbalances, several altered regions with high aberration frequencies were also refined when compared directly with other SNP/BAC array-based studies. For example, a study by Ross et al. (2007) delineated an overlapping region around 6q13-16 deletion measuring ~14 Mb, whereas Schwaenen et al. (2009) refined the deletion to ~9 Mb. Our analysis further reduced the region to ~34 kb, although this area does not correspond to any known gene. Delineation of the 1p36.3 terminal deletion has been a constant quest and the smallest reported to date was ~4 Mb in size (Martinez-Climent et al., 2003). We observed a ~2 Mb overlapping deletion in band 1p36.33-p36.32, containing 36 putative genes including the tumor suppressor *TP73*. However, sequence analysis has not shown any mutation (Ross et al., 2007). Lastly, the smallest detectable 10q23 deletion from our analysis was ~1.4 Mb, compared with ≥26 Mb in other studies (Cheung et al., 2009; Schwaenen et al., 2009). This region contains 10 genes including *CYP26A1*, *IDE*, *HHEX*, *FER1L3*, *CPEB3*, *MARCH5*, *EXOC6*, *KIF11*, *CYP26C1*, and *BTAF1*.

The most striking finding in this study was the observation that 45 of the 298 SNP-detected copy number imbalances affected single genes. The specificity of these aberrations prompted us to examine their significance in the cellular pathways context. It is known that molecular alterations associated with FL are heterogeneous and thus far no known single genetic defect has been shown to be responsible for progression and

Figure 3. Sensitivity of microaberration detection by BAC array CGH and 500K SNP. A: Side-by-side comparison between BAC array and SNP data in three regions, 12q (left panel), 1pter, and 1q (middle panel) and two 10q regions (right panel). B: The inability of software to identify single BAC shifts and ambiguous regions was demonstrated in representative regions that contained the *CDKN2A, PTPRD, TCRG, FHIT, KIT*, and *PEX14* genes. These regions were, however, verified by the apparent log ratio shifts in the same regions in the 500K SNP data. C: Shown here are representative FISH-validated cases with 9p21 and 10q23.3 deletions, two areas with relatively high frequencies of copy number aberrations detected by SNP arrays. Red dots represent the probes for 9p21 or 10q23.3 and green dots represent the control probes. Nuclei showing homozygous deletion of 9p21 and heterozygous deletion of 10q23, respectively, are indicated. D: Six representative examples single genes affected by regional aberrations are shown. Each panel shows the gene that overlapped with the computational calls (blue indicates loss; red indicates gain) and the corresponding SNP data points represented by black dots. The gene structure is divided into exons (represented by vertical bars) and introns (represented by lines between exons).

TABLE 2. Data from 500K SNP on the 45 regions that Affected 40 Unique Single Genes in the 25 FL Cohort (Data Based on NCBI Build 36.1)

Chr	Start bp	End bp	Cytoband	Length bp	Case ID	Aberration	No. markers	Gene
1	10469639	10595536	1p36.22	125,898	25	Gain	33	*PEX14*
1	72235233	72312983	1p31.1	77,751	2	Deletion	24	*NEGR1*
1	117834156	117888214	1p12	54,059	2	Deletion	10	*MAN1A2*
2	24268235	24316858	2p23.3	48,624	9	Gain	10	*ITSN2*
2	212857827	212892504	2q34	34,678	2	Deletion	15	*ERBB4*
3	60280769	60289134	3p14.2	8,366	18	Deletion	11	*FHIT*
3	60418812	60471672	3p14.2	52,861	10	Deletion	31	*FHIT*
3	60538690	60724747	3p14.2	186,058	25	Deletion	59	*FHIT*
3	61073569	61401584	3p14.2	328,016	25	Gain	62	*FHIT*
3	122381154	122576674	3q13.33	195,521	17	Deletion	11	*STXBP5L*
3	124316500	124368537	3q21.1	52,038	10	Deletion	17	*PDIA5*
3	178261992	178932509	3q26.32	670,518	11	Deletion	118	*TBL1XR1*
3	188960963	190139317	3q27.3–3q28	1,178,355	11	Deletion	255	*LPP*
4	55125451	55260088	4q12	134,638	17	Deletion	32	*KIT*
4	55260088	55506134	4q12	246,047	17	Gain	52	*KIT*
4	154752384	154787342	4q31.3	34,959	15	Gain	14	*KIAA0922*
5	75876017	75931436	5q13.3	55,420	1	Gain	12	*IQGAP2*
5	110695309	110729966	5q22.1	34,658	2	Deletion	10	*CAMK4*
5	158185416	158235128	5q33.3	49,713	5	Deletion	17	*EBF1*
5	160821706	160901217	5q34	79,512	2	Deletion	10	*GABRB2*
6	32496619	32536673	6p21.32	40,055	24	Deletion	20	*HLA-DRA*
6	55469594	55480711	6p12.1	11,118	2	Deletion	13	*HMGCLL1*
6	91292212	93604798	6q15–6q16.1	2,312,587	1	Gain	376	*MAP3K7*
6	166950588	166977470	6q27	26,883	7	Deletion	10	*RPS6KA2*
7	11674978	11733560	7p21.3	58,583	2	Deletion	15	*THSD7A*
7	14055006	14303956	7p21.2	248,951	5	Gain	70	*DGKB*
8	56913732	57061234	8q12.1	147,503	10	Deletion	39	*LYN*
8	113961782	114096174	8q23.3	134,393	2	Deletion	22	*CSMD3*
9	638996	645341	9p24.3	6,346	9	Gain	14	*KANK1*
9	8475988	8725832	9p24.1	249,845	8	Deletion	56	*PTPRD*
9	10303067	11202698	9p23	899,632	21	Deletion	173	*PTPRD*
9	21856815	21980324	9p21.3	123,510	13	Deletion	17	*CDKN2A*
9	21869702	22074610	9p21.3	204,909	15	Deletion	44	*CDKN2A CDKN2B*
10	97185573	97263800	10q23.33	78,228	5	Gain	15	*SORBS1*
10	108320750	108676711	10q25.1	355,962	8	Deletion	89	*SORCS1*
11	55391736	55429783	11q11	38,048	6	Gain	10	*SPRYD5*
12	23087336	23730505	12p12.1	643,170	8	Deletion	103	*SOX5*
12	97923776	98115559	12q23.1	191,784	8	Deletion	35	*ANKS1B*
12	120037518	120059343	12q24.31	21,826	10	Deletion	11	*P2RX7*
13	37220266	37261582	13q13.3	41,317	2	Deletion	13	*TRPC4*
13	69319666	69423324	13q21.33	103,659	20	Deletion	21	*KLHL1*
13	90565028	91431595	13q31.3	866,568	5	Gain	187	*GPC5*
16	69466000	69735178	16q22.2	269,179	13	Gain	18	*HYDIN*
17	28400243	28445879	17q11.2	45,637	5	Gain	15	*ACCN1*
18	51181107	51337548	18q21.2	156,442	19	Deletion	33	*TCF4*

Chr, chromosome.

transformation-related events that occur in all or the majority of patients (Lossos, 2005). As such, it has been postulated that different alterations in the same regulatory pathway(s) may be the driving force behind disease progression. For instance, a number of studies have examined the presence of aberrations that are unique to post-transformation FL or primary DLBCL specimens and found that mutations in *TP53* were detected in only one quarter of the cases (Lo Coco et al., 1993; Sander et al., 1993; Ichikawa et al., 1997; Koduru et al., 1997). As MDM2 is a key player in the regulation of TP53 by targeting it for proteasome degradation, Davies et al. (2005) evaluated the expression of MDM2 and showed that over expression of this protein in 17 of the 20 (75%) transformed paired specimens did not correlate with the status of TP53 gene mutation. These findings and others highlight the need to perform sophisticated pathway analysis to expand our

understanding of how different genes, often sharing similar functions and interacting pathways, may contribute to FL development and eventual transformation. In our analysis, these targeted genes were found to be significantly overrepresented in pathways categorized by the Ingenuity pathways analysis as important for "cancer," "cell death," "cellular growth," and "hematological disease." The two genes that are particularly critical in defining these pathways are *CDKN2A* and *CDKN2B*. Previous studies showed that there are three major cell cycle pathways involving the CDKN2A/B proteins: cyclin D-CDK4-RB, $p14^{ARF}$-MDM2-TP53-$p21^{CIP1}$, and $p27^{KIP1}$-cyclin E-CDK2. Alteration in any one of them may be an important marker of lymphoma progression, irrespective of histological grade (Sanchez-Beato et al., 2003). This cell cycle disruption not only confers a proliferative advantage to tumor cells but may also contribute to resistance to chemotherapy. *CDKN2A* has been reported to be the second most frequently altered gene in human malignancies after *TP53* (Hayslip and Montero, 2006). It is often codeleted with *CDKN2B*, likely due to their close proximity (Herman et al., 1997). Studies have consistently reported that *CDKN2A* aberrations, usually in the form of 9p21 deletion, LOH or promoter hypermethylation, are generally infrequent in B-cell lymphomas with low growth fraction (<5%), whereas inactivation of this gene can occur in as many as 50% of high-growth fraction tumors or aggressive variants such as DLBCL (Koduru et al., 1995; Ogawa et al., 1995; Uchida et al., 1995; Pinyol et al., 1998; Sanchez-Beato et al., 2001). Our findings showing targeted homozygous deletion of *CDKN2A* alone in one case and both *CDKN2A* and *CDKN2B* in another demonstrate possible involvement of these genes in contributing to FL development or progression in a portion of patients. In this regard, a recent study by Schwaenen et al. (2009) showed an unexpected high proportion (~13%) of 118 FL cases displaying deletion at 9p21 with a minimally affected region of 430 kb that corresponded exactly to the genomic location of *CDKN2A* and *CDKN2B* (Schwaenen et al., 2009). As multivariate analysis associated the 9p21 deletions with inferior clinical outcome, it was suggested that this region may constitute a new genomic prognostic marker for identifying FL patients with a propensity for transformation to aggressive disease (Schwaenen et al., 2009). Although correlation of 9p21 loss with clinical outcome could not be performed statistically due to small sample size in our study, we observed that of the three patients with a 9p homozygous deletion, one patient remains alive and two are deceased from transformation (67%), compared with five deaths in the other 22 cases that did not show the homozygous loss of 9p (23%). These data further support the importance of 9p21/CDKN2A/2B loss in survival.

Other single genes affected by copy number alterations in this study that warrant further analysis are *KIT*, *FHIT*, *PEX14*, and *PTPRD*, which have been previously linked to both hematological malignancies and solid tumors (Gavva et al., 2002; Chen et al., 2004; Kameoka et al., 2004; Zimpfer et al., 2004; Zhao et al., 2006; Purdie et al., 2007). Of particular interest, our SNP results show in one case (no. 17) a deletion in the first half and a gain in the 3′ portion of the *KIT* gene. Although sequence data would be needed to decipher the precise boundaries of the aberrations in the gene, based on our SNP data, the gain of the 3′ portion of *KIT* may affect the catalytic domain while the deleted portion may remove parts of the ligand binding/dimerization domain. In fact, the majority of the "gain-of-function" mutations of *KIT* have been documented to be concentrated around the 3′ portion from exon 11 to 18. This results in oncogenic activation of the SFK/STAT, Rac/Rho-JNK, Ras/MAP kinase, and PI3K/AKT signaling networks, causing decreased apoptosis and increased proliferation (Pekarsky et al., 2002; Scheijen and Griffin 2002; Al Kuraya et al., 2006; Lasota and Miettinen 2008). The aberrations we found in the *FHIT* gene are also of interest. The genomic structure of *FHIT* spans ~2 Mb and contains 10 small exons separated by large introns (Pekarsky et al., 2002). Its protein product has the ability to hydrolyze diadenosine nucleotides into ADP and AMP, however, this function has not been found to be linked to its tumor suppressive activities. Although presently not clear as to how the different types of mutations (including deletions and gains) of *FHIT* play a role in tumorigenesis, at least two recent studies have shown that microdeletions within the gene, similar to those found in three cases (nos. 10, 18, and 25) of our study, result in the selective loss of certain exons, which can cause aberrant RNA expression in diffuse large B-cell lymphoma (Kameoka et al., 2004; Al Kuraya et al., 2006). The potential significance of single genes altered in only individual cases in this study, and whether they represent passenger or driver mutations, would require further

verification and evaluation in a larger cohort of lymphomas.

Our analysis also identified two potential canonical pathways involving Wnt/β-catenin signaling and G1/S checkpoint regulation that were most significant to our single gene data set. The association between *CDKN2A* and *CDKN2B* with the regulation of the G1 checkpoint pathway is well established. The role of the Wnt/β-catenin signaling pathway, on the other hand, has only been described in CML, acute lymphoblastic leukemia, chronic lymphocytic leukemia, multiple myeloma and in mice predisposed for developing myeloid and lymphoid leukemias (Lu et al., 2004; Nemeth and Bodine, 2007; Schmidt et al., 2009). Wnt/β-catenin signaling, through a series of proteins such as the SOX family transcription factors, the TCF DNA-binding proteins and the MAP kinases, modulates cell fate and proliferation in many different adult and embryonic cells (Zorn et al., 1999; Schmidt et al., 2009). Enhanced activation of this pathway has been reported in the malignancies mentioned above. Further studies will be required to validate the mechanism by which these genes may impact the process of FL tumorigenesis.

In summary, this study has shown the advantage of using three interrogative methods, namely karyotyping, array CGH, and the 500K SNP set, to investigate balanced translocations, copy number imbalances, and cnLOH and to provide cross validation. To the best of our knowledge, this is the first study that has examined FL biopsies with matched normal tissues using a combination of high array technologies to identify somatic changes. We have taken the approach of focusing on regional aberrations that target single genes and found common pathways in which they participate, highlighting the possibility that in at least certain cases, different genes in the same pathways can be disrupted to give rise to the same clinical disease phenotype.

ACKNOWLEDGMENTS

The authors thank Suzanne Chan, Jennifer Asano, and Adrian Ally for expert assistance with SNP arrays. The laboratory work was undertaken at the Genome Sciences Center, British Columbia Cancer Research Center and the Center for Translational and Applied Genomics, a program of the Provincial Health Services Authority Laboratories.

REFERENCES

Al Kuraya K, Siraj AK, Bavi P, Al-Jomah N, El-Solh H, Ezzat A, Al-Dayel F, Belgaumi A, Al-Kofide A, Sabbah R, Sheikh S, Amr S, Simon R, Sauter G. 2006. High throughput tissue microarray analysis of FHIT expression in diffuse large cell B-cell lymphoma from Saudi Arabia. Mod Pathol 19:1124–1129.

Au WY, Gascoyne RD, Viswanatha DS, Skinnider BF, Connors JM, Klasa RJ, Horsman DE. 1999. Concurrent chromosomal alterations at 3q27, 8q24 and 18q21 in B-cell lymphomas. Br J Haematol 105:437–440.

Barbieri D, Michaux JL, Bosly A, van Hove W, Noens L, Drochmans A, Louwagie A, Tricot G, Boogaerts M, Vermaelen K. 1984. Cytogenetic evaluation of bone marrow involvement in non-Hodgkin's lymphomas. A survey of 94 cases. Haematologica 69:285–296.

Bende RJ, Smit LA, van Noesel CJ. 2007. Molecular pathways in follicular lymphoma. Leukemia 21:18–29.

Benjamini Y, Liu W. 1999. A step-down multiple hypotheses testing procedure that controls the false discovery rate under independence. J Stat Plan Inference 82:163–170.

Chen PM, Yang MH, Hsiao LT, Yu IT, Chu CJ, Chao TC, Yen CC, Wang WS, Chiou TJ, Liu JH. 2004. Decreased FHIT protein expression correlates with a worse prognosis in patients with diffuse large B-cell lymphoma. Oncol Rep 11: 349–356.

Cheung KJ, Shah SP, Steidl C, Johnson N, Relander T, Telenius A, Lai B, Murphy KP, Lam W, Al-Tourah AJ, Connors JM, Ng RT, Gascoyne RD, Horsman DE. 2009. Genome-wide profiling of follicular lymphoma by array comparative genomic hybridization reveals prognostically significant DNA copy number imbalances. Blood 113:137–148.

Davies AJ, Lee AM, Taylor C, Clear AJ, Goff LK, Iqbal S, Cuthbert-Heavens D, Calaminici M, Norton AJ, Lister TA, Fitzgibbon J. 2005. A limited role for TP53 mutation in the transformation of follicular lymphoma to diffuse large B-cell lymphoma. Leukemia 19:1459–1465.

de Leeuw RJ, Davies JJ, Rosenwald A, Bebb G, Gascoyne RD, Dyer MJ, Staudt LM, Martinez-Climent JA, Lam WL. 2004. Comprehensive whole genome array CGH profiling of mantle cell lymphoma model genomes. Hum Mol Genet 13:1827–1837.

Dolken G, Illerhaus G, Hirt C, Mertelsmann R. 1996. BCL-2/JH rearrangements in circulating B cells of healthy blood donors and patients with nonmalignant diseases. J Clin Oncol 14:1333–1344.

Fitzgibbon J, Iqbal S, Davies A, O'shea D, Carlotti E, Chaplin T, Matthews J, Raghavan M, Norton A, Lister TA, Young BD. 2007. Genome-wide detection of recurring sites of uniparental disomy in follicular and transformed follicular lymphoma. Leukemia 21:1514–1520.

Gavva NR, Wen SC, Daftari P, Moniwa M, Yang WM, Yang-Feng LP, Seto E, Davie JR, Shen CK. 2002. NAPP2, a peroxisomal membrane protein, is also a transcriptional corepressor. Genomics 79:423–431.

Hayslip J, Montero A. 2006. Tumor suppressor gene methylation in follicular lymphoma: A comprehensive review. Mol Cancer 5:44.

Herman JG, Civin CI, Issa JP, Collector MI, Sharkis SJ, Baylin SB. 1997. Distinct patterns of inactivation of p15INK4B and p16INK4A characterize the major types of hematological malignancies. Cancer Res 57:837–841.

Horsman DE, Connors JM, Pantzar T, Gascoyne RD. 2001. Analysis of secondary chromosomal alterations in 165 cases of follicular lymphoma with t(14;18). Genes Chromosomes Cancer 30: 375–382.

Ichikawa A, Kinoshita T, Watanabe T, Kato H, Nagai H, Tsushita K, Saito H, Hotta T. 1997. Mutations of the p53 gene as a prognostic factor in aggressive B-cell lymphoma. N Engl J Med 337:529–534.

Ishkanian AS, Malloff CA, Watson SK, DeLeeuw RJ, Chi B, Coe BP, Snijders A, Albertson DG, Pinkel D, Marra MA, Ling V, MacAulay C, Lam WL. 2004. A tiling resolution DNA microarray with complete coverage of the human genome. Nat Genet 36:299–303.

Johnson NA, Al-Tourah A, Brown CJ, Connors JM, Gascoyne RD, Horsman DE. 2008. Prognostic significance of secondary cytogenetic alterations in follicular lymphomas. Genes Chromosomes Cancer 47:1038–1048.

Johnson NA, Boyle M, Bashashati A, Leach S, Brooks-Wilson A, Sehn LH, Chhanabhai M, Brinkman RR, Connors JM, Weng

AP, Gascoyne RD. 2009. Diffuse large B-cell lymphoma: Reduced CD20 expression is associated with an inferior survival. Blood 113:3773–3780.
Kameoka Y, Tagawa H, Tsuzuki S, Karnan S, Ota A, Suguro M, Suzuki R, Yamaguchi M, Morishima Y, Nakamura S, Seto M. 2004. Contig array CGH at 3p14.2 points to the FRA3B/FHIT common fragile region as the target gene in diffuse large B-cell lymphoma. Oncogene 23:9148–9154.
Koduru PR, Raju K, Vadmal V, Menezes G, Shah S, Susin M, Kolitz J, Broome JD. 1997. Correlation between mutation in P53, p53 expression, cytogenetics, histologic type, and survival in patients with B-cell non-Hodgkin's lymphoma. Blood 90: 4078–4091.
Koduru PR, Zariwala M, Soni M, Gong JZ, Xiong Y, Broome JD. 1995. Deletion of cyclin-dependent kinase 4 inhibitor genes P15 and P16 in non-Hodgkin's lymphoma. Blood 86:2900–2905.
Krug U, Ganser A, Koeffler HP. 2002. Tumor suppressor genes in normal and malignant hematopoiesis. Oncogene 21:3475–3495.
Krzywinski M, Bosdet I, Smailus D, Chiu R, Mathewson C, Wye N, Barber S, Brown-John M, Chan S, Chand S, Cloutier A, Girn N, Lee D, Masson A, Mayo M, Olson T, Pandoh P, Prabhu AL, Schoenmakers E, Tsai M, Albertson D, Lam W, Choy CO, Osoegawa K, Zhao S, de Jong PJ, Schein J, Jones S, Marra MA. 2004. A set of BAC clones spanning the human genome. Nucleic Acids Res 32:3651–3660.
Lasota J, Miettinen M. 2008. Clinical significance of oncogenic KIT and PDGFRA mutations in gastrointestinal stromal tumours. Histopathology 53:245–266.
Limpens J, Stad R, Vos C, de Vlaam C, de Jong D, van Ommen GJ, Schuuring E, Kluin PM. 1995. Lymphoma-associated translocation t(14;18) in blood B cells of normal individuals. Blood 85:2528–2536.
Lo Coco F, Gaidano G, Louie DC, Offit K, Chaganti RS, Dalla-Favera R. 1993. P53 Mutations are associated with histologic transformation of follicular lymphoma. Blood 82:2289–2295.
Lossos IS. 2005. Higher-grade transformation of follicular lymphoma—A continuous enigma. Leukemia 19:1331–1333.
Lu D, Zhao Y, Tawatao R, Cottam HB, Sen M, Leoni LM, Kipps TJ, Corr M, Carson DA. 2004. Activation of the Wnt signaling pathway in chronic lymphocytic leukemia. Proc Natl Acad Sci USA 101:3118–3123.
Martinez-Climent JA, Alizadeh AA, Segraves R, Blesa D, Rubio-Moscardo F, Albertson DG, Garcia-Conde J, Dyer MJ, Levy R, Pinkel D, Lossos IS. 2003. Transformation of follicular lymphoma to diffuse large cell lymphoma is associated with a heterogeneous set of DNA copy number and gene expression alterations. Blood 101:3109–3117.
McDonnell TJ, Deane N, Platt FM, Nunez G, Jaeger U, McKearn JP, Korsmeyer SJ. 1989. bcl-2-immunoglobulin transgenic mice demonstrate extended B cell survival and follicular lymphoproliferation. Cell 57:79–88.
McDonnell TJ, Korsmeyer SJ. 1991. Progression from lymphoid hyperplasia to high-grade malignant lymphoma in mice transgenic for the t(14; 18). Nature 349:254–256.
Mecucci C, Vermaelen K, Tricot G, Louwagie A, Michaux JL, Bosly A, Thomas J, Barbieri D, Van den Berghe H. 1983. 3q-, 3q+ Anomaly in malignant proliferations in humans. Cancer Genet Cytogenet 9:376–381.
Nemeth MJ, Bodine DM. 2007. Regulation of hematopoiesis and the hematopoietic stem cell niche by Wnt signaling pathways. Cell Res 17:746–758.
Ogawa S, Hangaishi A, Miyawaki S, Hirosawa S, Miura Y, Takeyama K, Kamada N, Ohtake S, Uike N, Shimazaki C. 1995. Loss of the cyclin-dependent kinase 4-inhibitor (p16; MTS1) gene is frequent in and highly specific to lymphoid tumors in primary human hematopoietic malignancies. Blood 86:1548–1556.
O'shea D, O'Riain C, Gupta M, Waters R, Yang Y, Wrench D, Gribben J, Rosenwald A, Ott G, Rimsza LM, Holte H, Cazier JB, Johnson NA, Campo E, Chan WC, Gascoyne RD, Young BD, Staudt LM, Lister TA, Fitzgibbon J. 2009. Regions of acquired uniparental disomy at diagnosis of follicular lymphoma are associated with both overall survival and risk of transformation. Blood 113:2298–2301.
Pekarsky Y, Zanesi N, Palamarchuk A, Huebner K, Croce CM. 2002. FHIT: From gene discovery to cancer treatment and prevention. Lancet Oncol 3:748–754.
Pinyol M, Cobo F, Bea S, Jares P, Nayach I, Fernandez PL, Montserrat E, Cardesa A, Campo E. 1998. p16(INK4a) gene inactivation by deletions, mutations, and hypermethylation is associated with transformed and aggressive variants of non-Hodgkin's lymphomas. Blood 91:2977–2984.
Purdie KJ, Lambert SR, Teh MT, Chaplin T, Molloy G, Raghavan M, Kelsell DP, Leigh IM, Harwood CA, Proby CM, Young BD. 2007. Allelic imbalances and microdeletions affecting the PTPRD gene in cutaneous squamous cell carcinomas detected using single nucleotide polymorphism microarray analysis. Genes Chromosomes Cancer 46:661–669.
Ross CW, Ouillette PD, Saddler CM, Shedden KA, Malek SN. 2007. Comprehensive analysis of copy number and allele status identifies multiple chromosome defects underlying follicular lymphoma pathogenesis. Clin Cancer Res 13:4777–4785.
Sanchez-Beato M, Saez AI, Navas IC, Algara P, Sol Mateo M, Villuendas R, Camacho F, Sanchez-Aguilera A, Sanchez E, Piris MA. 2001. Overall survival in aggressive B-cell lymphomas is dependent on the accumulation of alterations in p53, p16, and p27. Am J Pathol 159:205–213.
Sanchez-Beato M, Sanchez-Aguilera A, Piris MA. 2003. Cell cycle deregulation in B-cell lymphomas. Blood 101:1220–1235.
Sanchez-Izquierdo D, Siebert R, Harder L, Marugan I, Gozzetti A, Price HP, Gesk S, Hernandez-Rivas JM, Benet I, Sole F, Sonoki T, Le Beau MM, Schlegelberger B, Dyer MJ, Garcia-Conde J, Martinez-Climent JA. 2001. Detection of translocations affecting the BCL6 locus in B cell non-Hodgkin's lymphoma by interphase fluorescence in situ hybridization. Leukemia 15:1475–1484.
Sander CA, Yano T, Clark HM, Harris C, Longo DL, Jaffe ES, Raffeld M. 1993. P53 Mutation is associated with progression in follicular lymphomas. Blood 82:1994–2004.
Scheijen B, Griffin JD. 2002. Tyrosine kinase oncogenes in normal hematopoiesis and hematological disease. Oncogene 21:3314–3333.
Schmidt M, Sievers E, Endo T, Lu D, Carson D, Schmidt-Wolf IG. 2009. Targeting Wnt pathway in lymphoma and myeloma cells. Br J Haematol 144:796–798.
Schwaenen C, Viardot A, Berger H, Barth TF, Bentink S, Dohner H, Enz M, Feller AC, Hansmann ML, Hummel M, Kestler HA, Klapper W, Kreuz M, Lenze D, Loeffler M, Moller P, Muller-Hermelink HK, Ott G, Rosolowski M, Rosenwald A, Ruf S, Siebert R, Spang R, Stein H, Truemper L, Lichter P, Bentz M, Wessendorf S, Molecular Mechanisms in Malignant Lymphomas Network Project of the Deutsche Krebshilfe. 2009. Microarray-based genomic profiling reveals novel genomic aberrations in follicular lymphoma which associate with patient survival and gene expression status. Genes Chromosomes Cancer 48:39–54.
Shah SP, Lam WL, Ng RT, Murphy KP. 2007. Modeling recurrent DNA copy number alterations in array CGH data. Bioinformatics 23:i450–i458.
Shah SP, Xuan X, DeLeeuw RJ, Khojasteh M, Lam WL, Ng R, Murphy KP. 2006. Integrating copy number polymorphisms into array CGH analysis using a robust HMM. Bioinformatics 22:e431–e439.
Swerdlow SH, Campo E, Harris NL, Jaffe ES, Pileri SA, Stein H, Thiele J, Vardiman JW, editors. 2008. WHO Classification of Tumours of Haematopoietic and Lymphoid Tissue (IARC WHO Classification of Tumours), 4th ed. World Health Organization, Lyon, 439 p.
Tilly H, Rossi A, Stamatoullas A, Lenormand B, Bigorgne C, Kunlin A, Monconduit M, Bastard C. 1994. Prognostic value of chromosomal abnormalities in follicular lymphoma. Blood 84: 1043–1049.
Tyybakinoja A, Elonen E, Vauhkonen H, Saarela J, Knuutila S. 2008. Single nucleotide polymorphism microarray analysis of karyotypically normal acute myeloid leukemia reveals frequent copy number neutral loss of heterozygosity. Haematologica 93: 631–632.
Uchida T, Watanabe T, Kinoshita T, Murate T, Saito H, Hotta T. 1995. Mutational analysis of the CDKN2 (MTS1/p16ink4A) gene in primary B-cell lymphomas. Blood 86:2724–2731.
Zhao P, Lam AK, Lu YL, Zhong M, Chen LH, Pu XL. 2006. Aberrant FHIT protein expression in classical Hodgkin's lymphoma: A potential marker. Pathology 38:399–402.
Zimpfer A, Went P, Tzankov A, Pehrs AC, Lugli A, Maurer R, Terracciano L, Pileri S, Dirnhofer S. 2004. Rare expression of KIT (CD117) in lymphomas: A tissue microarray study of 1166 cases. Histopathology 45:398–404.
Zorn AM, Barish GD, Williams BO, Lavender P, Klymkowsky MW, Varmus HE. 1999. Regulation of Wnt signaling by Sox proteins: XSox17 alpha/beta and XSox3 physically interact with beta-catenin. Mol Cell 4:487–498.